Journal of Chromatography, 635 (1993) 51–60
Elsevier Science Publishers B.V., Amsterdam

CHROM. 24 843

Quantitation of non-ideal behavior in protein size-exclusion chromatography

Paul L. Dubin*, Shun L. Edwards and Mamta S. Mehta☆

Department of Chemistry, Indiana University, Purdue University at Indianapolis, Indianapolis, IN 46205 (USA)

Donald Tomalia

Department of Chemistry and Macromolecular Architecture, the Michigan Molecular Institute, Midland, MI 48640 (USA)

(First received September llth, 1992; revised manuscript received November 6th, 1992)

ABSTRACT

The size-exclusion chromatographic partition coefficient (K_{SEC}) was measured on a Superose 6 column for three sets of well-characterized spherically symmetrical solutes: the compact, densely branched non-ionic polysaccharide, Ficoll; the flexible chain non-ionic polysaccharide, pullulan; and compact, anionic synthetic polymers, carboxylated starburst dendrimers. All three solutes display a congruent dependence of K_{SEC} on solute radius, *R*. In accord with a simple geometric model for SEC, all of these data conform to the same linear plot of $K_{SEC}^{1/2}$ *vs. R. This* plot reveals the behavior of non-interacting spheres on this column. Comparison of results for a number of globular proteins at various pH values to this "ideal" curve allows a quantitative measure of protein attraction or repulsion. It is shown that the usual procedure of obtaining a "best-fit" curve for a set of proteins is likely to generate an erroneous calibration curve.

INTRODUCTION

Size-exclusion chromatography (SEC) is an important liquid chromatographic technique for the separation of biopolymers [1,2]. Unlike other chromatographic methods, SEC has the potential of providing information about the molecular weight — or, to be more precise, the molecular size of the solute. It is possible to couple an SEC system to a "molecular weight detector"; then, the liquid chromatograph simply serves as the separation step prior to the analysis of the sample by, for example, light scattering. However, if the column is properly calibrated, the elution volume itself can be correlated with solute size, and hence, molar mass. This calibration is a difficult problem, because (a) the "standards" used in the calibration process must have the same relationship between molar mass and molar volume as the sample being analyzed, and (b) the separation process must be controlled solely by steric or entropic effects for both standards and analytes. The second requirement is particularly difficult in SEC of proteins, because each protein has a unique pattern of surface charge distribution and hydrophobicity. Despite great technological progress is preparing SEC packings that have relatively little hydrophobic character and relatively low surface charge [3,4], it is difficult to ensure that the chromatography of a series of proteins is not affected by the unique electrostatic or hydropho-

* Corresponding author.
☆ Present address: Department of Chemistry, University of Illinois at Urbana-Champaign, Urbana IL 61801, USA.

0021-9673/93/$06.00 © 1993 Elsevier Science Publishers B.V. All rights reserved

bic interactions of the individual proteins with the packing.

The general procedure for calibrating an SEC column for proteins consists of obtaining the dependence of either the retention volume (V_e) or the chromatographic partition coefficient (K_{SEC}) on either molecular weight or the diffusion-related Stokes radius (R_s). K_{SEC} is given by

$$K_{SEC} = (V_e - V_0)/(V_t - V_0) \quad (1)$$

where V_0 is the interstitial volume of the column, obtained as the retention volume of a solute too large to permeate the pores, and V_t is the total liquid volume of the column, obtained from the retention volume of a small solute, such as ^2H_2O, acetone or dextrose. There is some evidence that the diffusional Stokes radius does not unify the data for a variety of solutes as well as the viscosity radius [5]:

$$R_\eta = \{3([\eta]M_r)/10\pi N_A\}^{1/3} \quad (2)$$

(if the units of $[\eta]$ are cm^3/g, then R has units of cm) but for most globular proteins, R_η and R_s are identical, within experimental error [6]. (The frequent use of the term "hydrodynamic radius", which is ambiguous in that the relevant hydrodynamic property may be undefined, has had the unfortunate effect of confusing these two parameters.) However, when either R_s or R_η is plotted against V_e or K_{SEC}, the data typically display some scatter around the best-fit curve. It is usually not clear whether this scatter results from adsorptive or repulsive electrostatic interactions between solutes and stationary phase, arises from excess asymmetry of some of the standards (*i.e.* the set of standards does not represent a geometrically homologous series), or is a consequence of errors in the determination of V_e or R_s, *i.e.* true experimental error. In the absence of this information it is common practice to use the best-fit curve for calibration. This practice leads to a rather large uncertainty in the determination of the molecular mass of protein analytes.

A related problem arises when proteins are used to test SEC theories. In a geometric sense, R_s and R_η are much more clearly defined for proteins than are similar parameters for either flexible chain polymers or rod-like macromolecules. Therefore, data obtained for globular proteins have often been used to determine the validity of relationships between R and K resulting from different models of SEC [7–10]. The effects of adsorptive and repulsive interactions weaken the utility of such evaluations.

In the current work, we compare the retention behavior of proteins on a Superose 6 column to the elution of non-interacting spheres. The solutes that most closely approximate this behavior are fractions of Ficoll, a densely branched, highly compact, non-ionic polysaccharide prepared by polymerization of epichlorohydrin and sucrose [11,12]. Evidence in support of the compact spherical behavior of Ficoll comes from the Mark-Houwink exponent of a = 0.27 in the viscosity-MW relationship $[\eta] = KM^a$ [13], and also from measurements of its hindered diffusion through pores [14,15]. In addition to Ficoll, we also report here on the chromatography of carboxylated starburst dendrimers [16]. These solutes are even more impermeable than Ficoll, in view of the value of less than 0.1 [17]. Although these compounds are anionic, an electrolyte content greater than 0.4 M at neutral or acidic pH appears to fully suppress repulsive interactions with the weakly anionic Superose packing. A third solute studied is pullulan, a non-ionic linear polysaccharide [18]. Although the flexible chain structure of this polymer makes its dimensional measurement more ambiguous, a growing body of literature supports the observation that flexible chain molecules co-elute with compact or globular ones that have the same R_η [9,19,20], although there is still some disagreement on this point [21]. The goal of the present study is to determine whether such simple macromolecules can be used to define the "ideal" calibration curve for a given column -*i.e.* the dependence of K_{SEC} on R for non-interacting spheres. If this is the case, then deviations between this curve and the measured values for proteins can be interpreted more clearly than deviations between the best-fit curve for a series of proteins and the results for any apparent "outliers". It is then possible to determine which (if any) proteins exhibit ideal behavior, and to quantitatively determine the

magnitude of solute-packing interaction effects for those that do not.

EXPERIMENTAL

Materials

Table I lists the proteins employed in this study, along with their MW, isoelectric point, and Stokes radius and viscosity radius, where available. Ficoll fractions were a gift of Dr. K. Granath at Pharmacia Biotechnology, Uppsala, Sweden. Their characteristics are listed in Table II. Pullulan fractions were commercial materials obtained from Shodex Corp. (New York, NY, USA), with MW values and polydispersities shown in Table III. Also tabulated are Stokes radii and viscosity radii, measured as discussed below. Carboxylated starburst dendrimers, hereinafter referred to as "dendrimers", were prepared as described in ref. 16, and were characterized by dynamic light scattering and viscometry, as described elsewhere [26]. Values for their viscosity radii and Stokes radii are given in Table IV All buffers and salts were reagent grade, from Sigma, Mallinckrodt, Fisher or Aldrich.

Methods

Size-exclusion chromatography. SEC was carried out on a prepacked Superose 6 HR 10/30 column, which had a column efficiency of 3800-4600 plates/m throughout most of these studies.

TABLE I

CHARACTERISTICS OF PROTEINS USED IN THIS STUDY

Protein[a]	Source	Mw	*pI*	R_s (nm)	R_η (nm)
Ribonuclease (R-5503)	Bovine pancreas	13708	9.0	1.75 [22]	1.90 [6]
Lysozyme (L-6876)	Egg white	14000	11.0	1.85 [23]	2.0 [6]
Myoglobin (M-1882)	Horse heart	17 800	7.3	1.9 [22]	2.06 [6]
β-Lactoglobulin (L-2506)	Bovine milk	35 000	5.2	2.7 [24]	2.65 [6]
Albumin (A-7906)	Bovine serum	66000	4.9	3.5 [22,25]	3.4 [25]
y-Globulin (G-5009)	Bovine	150 000	7.0	5.6 [24]	–
Catalase (C-40)	Bovine liver	223 000	5.4	5.2 [22]	5.2 [6]
Apoferritin (A-3600)	Horse spleen	443000	5.0	6.1 [5,24]	6.1 [6]
Thyroglobulin (T-1001)	Bovine	669 000	5.1	8.6 [22]	7.9 [25]

[a] All from Sigma, except y-globulin also supplied by CalBiochem.

TABLE II

CHARACTERISTICS OF FICOLL FRACTIONS

Fraction	M_w, LS[a]	M_w, SEC[a]	M_n, SEC[a]	M_w/M_n[b]	$[\eta]$[c] (cm^3/g)	R_s[d] (nm)	R_η[e] (nm)
T1800, Fr. 9	714 000	644000	337 000	1.91	18.5	17	12.4
T1800, Fr. 12	461000	460000	257000	1.79	16.9	13	10.7
T1800, Fr. 15	321000	332 000	244 000	1.36	15.5	11	9.4
T1800, Fr. 20	132 000	134 000	113 700	1.18	12.1	7.1	6.4
T2580 IV B, Fr. 3	–	66 500	59 000	1.13	10.0	4.7	4.7
T2580 IV B, Fr. 11	–	21800	20300	1.07	7.4	3.0	3.0

[a] From supplier.
[b] M_w = Mass-average molecular mass; M_n = number-average molecular mass.
[c] Calculated from $[\eta] = 0.005 \cdot M_w^{0.27}$ [13].
[d] From measured diffusion coefficient.
[e] From columns 3 and 6, via eqn. (2).

TABLE III

CHARACTERISTICS OF PULLULAN STANDARDS

Sample	M_w [a]	M_w/M_n [a]	R_s (nm)[b]	$[\eta]$ (cm^3/g)	R_η (nm)[c]
Pullulan P-8a0	853 000	1.14	25.8	171	28.5
Pullulan P-400	380 000	1.12	17.6	105	18.5
Pullulan P-200	186000	1.13	12.8	55	11.8
Pullulan P-100	100000	1.10	8.8	39.8	8.6
Pullulan P-50	48000	1.09	6.1	23.4	5.6
Pullulan P-20	23700	1.07	4.0	15.5	3.9
Pullman P-10	12 200	1.06	3.0	9.70	2.7
Pullman P-5	5800	1.07	2.1	6.30	1.8

[a] From manufacturer.
[b] By QELS.
[c] In 0.20 *M* phosphate buffer (pH 7.0).
[d] From columns 2 and 5, via eqn. 2.

The HPLC instrument was a Beckmann System Gold, equipped with a Beckmann Model 156 refractive index detector or a Waters R401 differential refractive index detector, along with the UV detector supplied with the instrument. Solvent was delivered with a Beckmann 110 B pump and an Altex 210A valve with either a 20, 50 or 100 μl loop. A Rheodyne 0.2 μm precolumn filter was placed in-line to protect the column. Plow-rates were measured and found to be constant within ±0.5% by weighing of collected eluant. Sample preparation was accomplished by shaking or tumbling for l-2 h. The concentration of all polymers and proteins were in the range 2-5 mg/ml, except for concentration effect studies. Samples were filtered through 0.45 μm Gelman filters before injection. K_{SEC} was determined according to eqn. 1 with V_0 determined from the retention of either $2 \cdot 10^6$ MW dextran or $4 \cdot 10^6$ MW PEO as 6.50 ml, and V_t determined from the retention of dextrose as 19.98 ml.

TABLE IV

CHARACTERISTICS OF DENDRIMERS

Generation	MW"	R_s (nm)[b]	R_η (nm)
0.5	924	0.95	–
1.5	2173	1.3	–
2.5	4672	1.5	1.5
3.5	9670	2.5	1.9
4.5	19666	3.1	2.5
5.5	39 657	3.7	3.1
6.5	79 639	4.5	4.0
7.5	159 603	6.0	5.3

[a] Calculated from expected chemical structure.
[b] From diffusion coefficient, by dynamic light scattering.
[c] From ref. 17.

Quasielastic light scattering (QELS). Light scattering measurements were made using one of two systems. With a Brookhaven (Holtsville, NY, USA) system equipped with a 72 channel digital correlator (BI-2030 AT) and using a Jodon 15 mW He-Ne laser (Ann Arbor, MI, USA) QELS measurements were made at scattering angles from 30" to 150°. Samples at concentrations of *ca.* 2 mg/ml were filtered through 0.20 μm Acrodisc filters (Gelman) prior to analysis. Counts were typically collected for one hour. We obtained the homodyne intensity-intensity correlation function ***G(q,t), with q,*** the amplitude of the scattering vector, given by $q = (4\pi n/\lambda)\sin(\theta/2)$, where n is the refractive index of the medium, λ is the wavelength of the excitation light in a vacuum, and θ is the scattering angle. $G(q,t)$ is related to the electric field correlation function of concentration fluctuations $g(q,t)$ by:

$$G(q,t) = A[1 + bg(q,t)^2] \quad (3)$$

where A is the experimental baseline and b is the fraction of the scattered intensity arising from concentration fluctuations.

The diffusion coefficients were calculated using

$$D = \frac{\Gamma\lambda^2}{16\pi^2 \sin^2(\theta/2)} \quad (4)$$

where Γ is the reciprocal of the diffusion time constant, which is obtained from the slope of $\ln g^2(q,t)$ *vs.* t plots. The diffusion coefficient, D, is directly related to the Stokes radius, R_s, by Stokes' equation

$$D = \frac{kT}{6\pi\eta R_s} \quad (5)$$

where k is Boltzmann's constant, T is the absolute temperature and η is the viscosity of the solvent.

QELS was also carried out with an Oros (Biotage Co. Charlottesville, VA, USA) Model 801 "molecular weight detector" which employs a 30-mW solid-state 780 nm laser, and an avalanche photodiode detector. Samples were introduced into the 7-μl scattering cell (maintained at 26.5 ± 0.4°C) through 0.2 μm Anotec filters. 90° scattering data were analyzed via cumulants. There were no significant differences between the results obtained using the two instruments.

Viscometry. Measurements were made with a Schott AVSN automatic viscometer equipped with a 10-ml capacity glass Type 531 capillary viscometer, at 25.0 ± 0.02°C. Samples were dissolved in the appropriate solvent at concentrations ranging from 6 to 17 mg/ml and filtered through 0.45 μm Gehnan filters. Efflux times were obtained with precisions of ±0.05 s. Solute concentrations were adjusted so that the efflux time of the most concentrated solutions exceeded that of the solvent by 10–30%. Intrinsic viscosities were obtained by the usual extrapolation to zero solute concentration.

RESULTS AND DISCUSSION

Fig. 1 shows the dependence of K_{SEC} on solute radius for Ficoll, pullulan and dendrimers. The mobile phase for the first two solutes was 0.20 M NaH_2PO_4–Na_2HPO_4, pH 7.0. In order to ensure the suppression of electrostatic repulsive interactions between the dendrimer and the packing, the ionic strength of the mobile phase was increased to 0.30 M for that solute. For the first two solutes, we employ the viscosity radius,

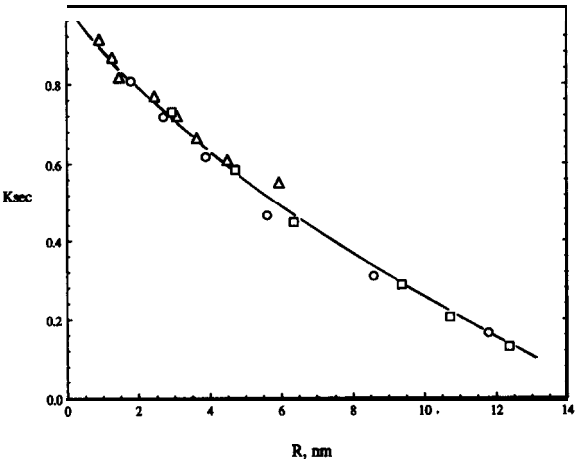

Fig. 1. Dependence of K_{SEC} on solute radius for (Cl) Ficoll. (0) pullulan, and (A) carboxylated starburst dendrimers, on Superose 6, in pH 7.0 phosphate buffer (0.20 M for Ficoll and pullulan, 0.30 M for dendrimers). Radii for dendrimers are Stokes radii from dynamic light scattering, all others are viscosity radii (see text for explanation).

obtained from eqn. 2 in conjunction with the intrinsic viscosity measured in the same solvent as the SEC mobile phase. In the case of Ficoll, the Stokes radii are substantially larger than the viscosity radii, particularly for the higher MW samples (see Table II). This result arises from the fact that QELS measures the z-average diffusion coefficient [27] which corresponds to a high moment of the distribution, so that R_s is skewed upward for the high M_w/M_n fractions. R_η corresponds better to the peak-eluting component and is therefore preferable, on these grounds at least. For the dendrimers, viscosity radii and Stokes' radii were measured in the mobile phase 0.38 M $NaNO_3$–NaH_2PO_4 (9:1) [17]. For dense spheres such as these dendrimers we should find $R_s = R_\eta$, as one in fact observes for proteins (*viz.* Table I), while for asymmetric solutes, R_η should be larger than R_s [21]. However, as shown in Table IV, we found the viscosity radii to be smaller than the corresponding Stokes' radii. We attribute this unreasonable result to the presence of low MW impurities (detectable by HPLC) which lead to incorrect estimates of the solute concentration and hence negative errors in $[\eta]$ (this hypothesis is also borne out by the scatter of the $\log[\eta]$–$\log M_r$ plot for the dendri-

mers [17]). These impurities have little effect, however, on the light scattering properties and we therefore employ the measured Stokes radii for the dendrimers.

As seen in Fig. 1, the congruence of the data for the three spherically symmetric solutes is very good. (The only severe deviation is observed for dendrimer G7.5. Since the measured R_s and R_η for this sample are consistent with the lower generation data, we believe these values are reliable, and are inclined to ascribe the result to incomplete carboxylation of this sample, leading to chromatographic adsorption. Such incomplete derivatization for these dendrimers has been noted elsewhere [28].) Furthermore, as previously found [26], the calibration curve so obtained for pullulan and Ficoll on Superose can be very well fitted to a theoretical expression based on the expected permeation of spherical solutes into a collection of somewhat polydisperse cylindrical cavities. It is of interest that the statistical coil nature of pullulan does not perturb its congruence with the more compact spheres. While flexible chains are anisotropic on very short time scales, this "breathing" motion is presumably so fast compared to translation over the length of a pore diameter, that the appropriate time average segment density is spherical. In any event, the good agreement between experiment and theory and the congruence of the data for the three solute sets leads us to identify the calibration curve of Fig. 1 with the behavior of non-interacting spheres.

For spherical solutes in a system of uniform cylindrical pores, K_{SEC} is given by [29,30]

$$K_{SEC} = (1 - R/r_p)^2 \qquad (6)$$

where R and r_p are the dimensions of solute and pore, respectively. (It must be recognized that for any real system, r_p represents a complex average of varying pore sizes and geometries.) A plot of $K_{SEC}^{1/2}$ *vs.* R should be a straight line with a slope of $1/r_p$ and an intercept of unity. Fig. 2 shows the results plotted according to eqn. 6. The data for Ficoll, dendrimers and pullulan conform remarkably well (correlation coefficient 0.993) to a straight line with an intercept of unity. The presence of a pore size distribution should in principle produce curvature in such

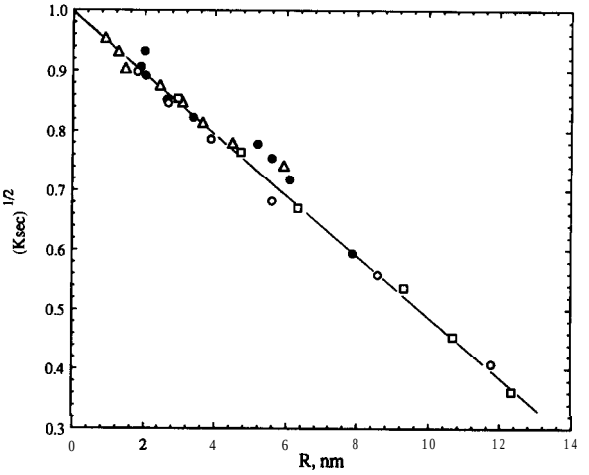

Fig. 2. Data of Fig. 1 plotted according to eqn. 3. Symbols as in Fig. 1, except (0): proteins in 0.50 *M* phosphate buffer (pH 7.0).

plots because the larger solutes sample a different pore size distribution than the smaller ones [26]. While these effects are significant for the present solute set on the lower-pore-size Superose 12 [26], the mean pore size of Superose 6 is much higher [31], *i.e.* twice the size of the biggest solutes studied here. The linearity of Fig. 2 suggests that all solutes sample a similar pore size distribution so that the effective mean pore radius is not solute size-dependent. It is also worth noting here that Waldmann-Meyer [30] did not find an intercept of unity for the elution of dextrans on porous glass and ascribed this

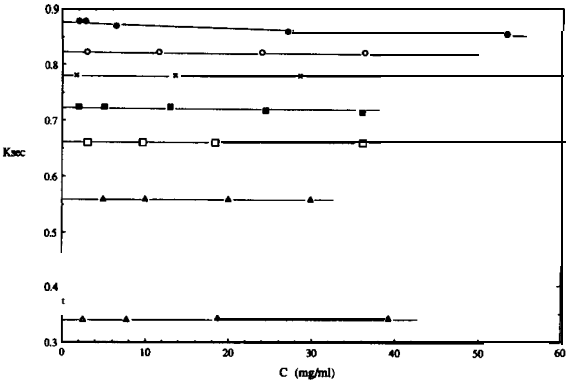

Fig. 3. Concentration dependence of K_{SEC} for proteins in pH 7.0 buffer. ● = Lysozyme; 0 = RNAse; x = myoglobin; ■ = β-lactoglobulin; □ = BSA; A = y-globulin; A = thyroglobulin.

effect to permeation of the V_t probe, $2H_2O$, into fissures in the packing material. The linear plot of Fig. 2 facilitates a comparison of the results for proteins to the "ideal" curve.

Fig. 2 also illustrates the deviations from the "ideal" curve for proteins. The values for K_{SEC} for the proteins, shown by the solid symbols in Fig. 2, correspond to the retention volumes measured under conditions of low protein-substrate interaction, *i.e. 0.50 M* phosphate buffer (pH 7.0). That the protein results are not influenced by aggregation effects is evident from Fig. 3, which shows that the concentration dependence of K_{SEC} for the proteins studied is negligible, with the possible exception of lysozyme. From Fig. 2 we observe that five of the nine proteins fall on the Ficoll/pullulan/dendrimer curve. Four others, however, elute relatively late. Thus, even neutral pH and a relatively high supporting electrolyte concentration do not ensure the suppression of adsorptive interactions. Given the very low hydrophobicity of Superose [32], it is probable that the adsorptive effects arise from electrostatic interactions with the carboxylic acid groups in the Superose. It is worth pointing out that, in the absence of the data for the synthetic polymers such as was obtained here, the standard procedure for calibration would be to draw the best fit line for the nine proteins. We believe that this would lead to systematic overestimate of the radius of non-adsorbing proteins, and that the error would be large if calibration were in terms of MW as opposed to radius.

At low pH and low ionic strength, the proteins all possess a positive net charge and we would expect the effects of adsorption to be amplified. This is seen in Fig. 4, where protein retentions at pH 4.3 and Z = 0.03 (lilled symbols) are compared to the "ideal" curve, which in this plot is transposed from Fig. 2. This process is justified by our finding that the calibration curve for pullulan is independent of pH or ionic strength, as shown in Fig. 5. It is certainly likely that electrostatic effects could be observed for carboxylated starburst dendrimers; since we conclude from Fig. 1 that, in principle, either Ficoll or pullulan fractions could serve to define the ideal dependence of K_{SEC} on R_s, and since the

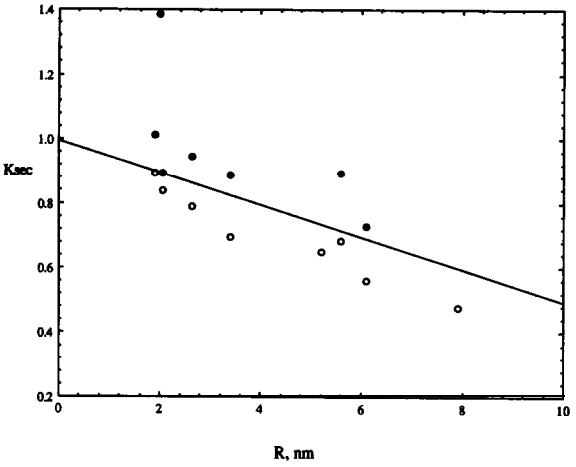

Fig. 4. Comparison of protein chromatography with "ideal" behavior. Solid line is transposed from Fig. 2. ● = Proteins in 0.03 *M* phosphate buffer (pH 4.3); 0 = proteins in 0.03 *M* phosphate buffer (pH 10.0).

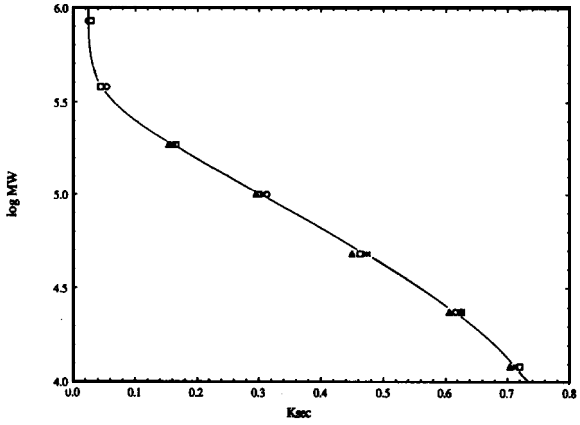

Fig. 5. Effect of ionic strength and pH on elution behavior of pullulan. (0) pH 7.0, Z = 0.1; (+) pH 10, Z = 0.1; (0) pH 4.3, $I = 0.1$; (A) pH 10, $I = 0.25$; (×) pH 7.0, $I = 0.25$.

pullulan chromatography is independent of pH and Z over a wide range, we believe the transposition of the "ideal curve" from one mobile phase to another is justifiable. At pH 4.3 and Z = 0.03 *M*, only one of the seven proteins tested falls on the ideal curve, with the other six showing significant positive departures from the expected K_{SEC} values. Conversely, at pH > isoelectric point, both proteins and packing bear a negative charge, and repulsive effects should be strong. The repulsive effect is dominant at high pH, as shown by the open symbols in Fig. 4

measured at I = 0.03 M and pH = 10.0. With the exception of RNase, all of the proteins elute before the ideal value of K_{SEC}.

Potschka [33] has noted similar effects for proteins on PW gel. Assuming that the plot of R_η *vs.* K_{SEC} obtained in pH 7.0, 100 mM phosphate buffer corresponded to ideal behavior, Potschka used this calibration curve along with the elution volume measured at higher pH to define an "effective R_η", which he interpreted as a sum of the geometric contribution from the protein and an electrostatic repulsion "length". By using neutral polymers to establish the ideal curve, we are less dependent on the assumption that all protein-packing interactions can be suppressed at some conditions, and the concomitant need to identify these conditions. The horizontal difference between the ideal curve and the measured R_η in Fig. 4 for the proteins at high pH is a similar measure of the contribution of electrostatic repulsion to K_{SEC}, and these values of AR are reported in Table V along with the net charge for those proteins where titration data are available. It is possible to interpret positive values of AR (in the repulsive regime) as an effective increase in protein size due to electrostatic repulsive forces [33] (although it is no more or less credible to assign the earlier elution to the electrical double layer on the surface of the packing [34]). On the other hand, negative values of AR (in the attractive regime) have no physical significance, and are included in Table V only for qualitative consideration.

The data in Table V, listed in order of decreasing protein pI, show the expected qualitative trends in the repulsive regime. At high pH, AR becomes more positive with decreasing isoelectric point. At neutral or low pH, the results are more complex. For example, RNase, β-lactoglobulin and BSA, with virtually identical net charges at pH = 4.3, exhibit differing excess retention, as represented by the negative values of AZ?. The magnitude of this quantity varies inversely with molecular mass, suggesting that the mean surface charge density might show better correlation with AR. In fact, the correlation coefficient between this last variable and Z/R^2 is found to be 0.99. On the other hand, the retention of lysozyme is clearly outside of this correlation. The data at neutral pH are even less amenable to this analysis, and it is difficult to account for the large retention of y-globulin and the nearly ideal behavior of BSA on the basis of net charge. These observations are consistent with the findings of Regnier and co-workers [35] who emphasized the role of the "charge patches" in controlling ion-exchange chromatography of proteins, and are analogous to our results for the association of proteins with oppositely charged soluble polyelectrolytes [36], in which the interaction appears to be dominated by some local (as opposed to global) charge density.

The current data base does not allow for a systematic investigation of the correlation of excess retention or repulsion effects with the local and global charge states of the protein. Efforts are currently underway to expand the chromatographic data set, using other proteins and acquiring the necessary pH–titration information. Attempts to correlate protein charge

TABLE V

PROTEIN NET CHARGES AND DISPLACEMENTS FROM IDEAL CURVE IN 0.03 *M* PHOSPHATE BUFFER

AR values are horizontal displacements from "ideal curve" in Fig. 4. Negative values correspond to excess retention, positive values to repulsion.

	pH = 4.3		pH = 7.0		pH = 10.0	
Protein	**Z**	**AR**	**Z**	**AR**	**Z**	**AR**
Lysozyme	+12	(< -30)	+7	(−7)	+3	0
RNase	+9	(-22)	+3	(−1)	- 3	(−1)
-y-Globulin	> +30	(-35)	0	(−7)	n.a.	8
β-Lactoglobulin	+8	(-15)	-18	+2	-36	17
BSA	+8	(-12)	-16	(−1)	-39	26

state with retention [37] will employ the computational and graphics capability of finite-element analysis programs, such as UHBD, developed for protein electrostatic modeling [38].

CONCLUSIONS

The dependence of K_{SEC} on the viscosity radius R for three spherically symmetrical synthetic polymers -Ficoll, pullulan and carboxylated dendrimers— conform to a single line which fits the expression $K_{SEC}^{1/2} = 1 - R/r_p$. At moderate ionic strength and neutral pH some globular proteins fall on this curve, which may be viewed as representing the chromatographic behavior of non-interacting spheres. Deviations from this curve may be identified with either significant departure from spherical symmetry, or solute-stationary phase interactions. The positive deviations seen for proteins at pH = 4.3 and Z = 0.03 M_r and the negative deviations for proteins at this ionic strength and at pH 10.0, indicate that these departures from the "ideal" curve arise from repulsive or attractive electrostatic interactions with the packing. By reference to the "ideal" curve these interactions may be measured quantitatively. The magnitude of the repulsive or attractive interactions do not correlate in any simple way with the protein net charge. This finding is consistent with the observation by Haggerty and Lenhoff [39] that the net protein charge does not allow any prediction of the ion-exchange capacity factor, and that the important variable is instead the mean surface potential of the protein.

ACKNOWLEDGEMENTS

Support from the National Science Foundation under Grant CHE-9021484 is gratefully acknowledged. We also thank Dr. K. Granath, of Pharmacia Biotechnology for providing the Ficoll fractions, and Dr. Lars Hagel, Pharmacia Biotechnology for the gift of a Superose column.

REFERENCES

1 K.M. Gooding, *Biochromatography,* 1 (1986) 34.
2 R.C. Montelaro, in P.L. Dubin (Editor), *Aqueous Size Exclusion Chromatography,* Elsevier, Amsterdam 1988, Ch. 10.
3 P.L. Dubin, *Adv. Chromatogr.*, *31* (1992) 122-125.
4 R.W.A. Oliver (Editor), *HPLC of Macromolecules, IRL* Press, Oxford, 1989, p. 5, 79.
5 P.J. Flory, *Principles of Polymer Chemistry,* Cornell University Press, Ithaca, NY, 1953, p. 606.
6 M. Potschka, *J. Chromatogr.*, submitted for publication.
7 T.C. Laurent and J. Killander, *J. Chromatogr., 14* (1964) 317.
8 G. Ackers, *J. Biol.* Chem., 242 (1967) 3237.
9 H. Waldmann-Meyer, *J. Chromatogr., 410 (1987) 233.*
10 M. le Maire, A. Ghazi, M. Martin and F. Brochard, *J. Biochem.,* 106 (1989) 814.
11 H. Holter and K.M. Meller, *Exp. Cell. Res.,* 15 (1956) 631.
12 T.C. Laurent and K. Granath, Biochim Biophys. *Acta, 136* (1967) *191.*
13 K. Granath, private communication.
14 M.P. Bohrer, G.D. Patterson and P.J. Carroll, *Macromolecules,* 17 (1984) 1170.
15 M.G. Davidson and W.M. Deen, *Macromolecules, 21 (1988) 3474.*
16 D.A. Tomalia, R.M. Naylor and W.A. Goddard, III, *Angew. Chem. Int. Ed. Engl., 29* (1990) 138.
17 P.L. Dubin, S.L. Edwards, J.I. Kaplan, M.S. Mehta, D. Tomalia and J. Xia, *Anal. Chem., 64 (1992) 2344.*
18 T. Kato, T. Okamoto, T. Tokuya and A. Takahashi, *Biopolymers, 21 (1982) 1623.*
19 R.P. Frigon, J.K. Leypoldt, S. Uyeji and L.W. Henderson, *Anal.* Chem., 55 (1983) 1349.
20 P.L. Dubin, B.A. Smith, J.M. Principi and M.A. Fallon, *J. Colloid Interface Sci., 127 (1989) 558.*
21 M. le Maire, A. Viel and J. Meller, *Anal. Biochem., 177 (1989) 50.*
22 M. le Maire, A. Ghazi, J.V. Møller and L.P. Aggerbeck, *Biochem. J., 243 (1987) 399.*
23 D. Nicoli and G. Benedek, *Biopolymers, 15 (1976) 2421.*
24 R.C. Tarvers and F.C. Church, *Int. J. Pept. Prot. Res., 26 (1985) 539.*
25 K. Horiike, H. Tojo, T. Yamano and M. Nozaki, *J. Biochem., 93 (1983) 99.*
26 S. Hussain, M.S. Mehta, J.I. Kaplan and P.L. Dubin, *Anal. Chem., 63* (1991) 1132.
27 G.D.J. Phillies, *Anal. Chem., 62* (1990) 1049A.
28 P. Russo, in preparation.
29 E.F. Casassa, *J. Phys.* Chem., 75 (1971) 275.
30 H. Waldmann-Meyer, *J. Chromatogr., 350 (1985) 1.*
31 L. Hagel, in P.L. Dubin (Editor), *Aqueous Size Exclusion* Chromatography, Elsevier, Amsterdam, 1988, Ch. 5.
32 P.L. Dubin and J.M. Principi, *Anal.* Chem., 61 (1989) 780.
33 M. Potschka, *J. Chromatogr.,* 441 (1988) 239.
34 P.L. Dubin, R.M. Latter, C.J. Wu and J.I. Kaplan, *J. Phys. Chem., 94* (1990) 7244.
35 W. Kopaciewicz, M.A. Rounds, J. Fausnaugh and F.E. Regnier, *J. Chromatogr., 266 (1983) 3.*

36 J.M. Park, B.B. Muhoberac, P.L. Dubin and J. Xia, *Macromolecules, 25 (1992) 290.*
37 P.L. Dubin, J. Klimkowski, J. Xia and Y. Zhu, in preparation.
38 M.E. Davis, J.D. Madura, B.A. Luty and J.A. McCammon, *Comp. Phys. Comm., 62* (1991) 187.
39 L. Haggerty and A.M. Lenhoff, *J. Phys. Chem., 95* (1991) 1472.